

DESY 09-033  
 SFB/CPP-09-26  
 LPT-ORSAY 09-17  
 HU-EP-09/12

# Lattice calculation of the Isgur-Wise functions $\tau_{1/2}$ and $\tau_{3/2}$ with dynamical quarks

Benoit Blossier<sup>a,b</sup>, Marc Wagner<sup>c</sup>, Olivier Pène<sup>b</sup>

<sup>a</sup> *DESY, Platanenallee 6, D-15738 Zeuthen, Germany*

<sup>b</sup> *Laboratoire de Physique Théorique (Bât.210), Université Paris-Sud XI,  
 Centre d'Orsay, 91405 Orsay-Cedex, France.*

<sup>c</sup> *Humboldt-Universität zu Berlin, Institut für Physik, Newtonstraße 15, D-12489 Berlin,  
 Germany*



March 13, 2009

---

## Abstract

We perform a dynamical lattice computation of the Isgur-Wise functions  $\tau_{1/2}$  and  $\tau_{3/2}$  at zero recoil. We consider three different light quark masses corresponding to  $300 \text{ MeV} \lesssim m_{\text{PS}} \lesssim 450 \text{ MeV}$ , which allow us to extrapolate our results to the physical  $u/d$  quark mass. We find  $\tau_{1/2}(1) = 0.296(26)$  and  $\tau_{3/2}(1) = 0.526(23)$ . Uraltsev's sum rule is saturated up to 80% by the ground state. We discuss implications regarding semileptonic decays  $B \rightarrow X_c l \nu$  and the associated "1/2 versus 3/2" puzzle.

---

# 1 Introduction

The semileptonic decay of  $B$  mesons into positive parity charmed mesons (often referred to as  $D^{**}$ 's) is an important and debated issue. Important, because no accurate measurement of the  $V_{cb}$  CKM angle will be possible, if these channels, which represent about one quarter of the semileptonic decays, are not well understood. Debated, because there seems to be a persistent discrepancy between claims from theory and from experiment [1].

Two types of  $D^{**}$ 's are seen, two “narrow resonances” and a couple of “broad resonances”, grossly speaking in the same mass region. While experiments point towards a dominance of the broad resonances in semileptonic decays, theory, when using the heavy quark limit, points rather towards a dominance of the narrow resonances. To clarify the situation ref. [1] called for actions on both the experimental and the theoretical side.

The theoretical argument relies on a series of sum rules [2, 3] derived from QCD comforted by model calculations [4, 5, 6]. Lattice calculations are needed to give a more quantitative prediction stemming directly from QCD. A preliminary computation was performed in [7], but only in quenched QCD and with a marginal signal-to-noise ratio. In this letter we report on the first unquenched computation using  $N_f = 2$  flavor gauge configurations with Wilson twisted quarks generated by the European Twisted Mass Collaboration (ETMC). The spectrum of heavy-light mesons in the static limit has already been reported [10, 11].

## 1.1 Spectrum in the heavy quark limit

We treat both  $b$  and  $c$  quarks via static Wilson lines, i.e. consider their infinite mass limit. In this limit the meson spectrum is constructed by combining the spin  $1/2$  of the heavy quark with the total angular momentum and parity  $j^P$  of the light degrees of freedom (light quarks and gluons) [12, 13, 14]. The two lightest negative parity mesons  $B$  and  $B^*$  (or  $D$  and  $D^*$ ) are degenerate and described by the same  $S \equiv (1/2)^-$  state of light particles. The lightest (non-radially excited) positive parity states can be decomposed into two degenerate doublets:  $P_- \equiv (1/2)^+$  and  $P_+ \equiv (3/2)^+$ . The total angular momenta  $J^P$  of the  $P_-$  ( $P_+$ ) mesons are  $0^+$ ,  $1^+$  ( $1^+$ ,  $2^+$ ). The mixing between the two  $1^+$  states is suppressed in the heavy quark limit.

It is generally believed that the narrow (broad) resonances are of the  $P_+$  ( $P_-$ ) type, since in the heavy quark limit they decay into  $D^{(*)}\pi$  via a  $D$  ( $S$ ) wave. The  $D$  wave decays are supposed to be suppressed by a centrifugal barrier, if the final state momenta are not too large.

## 1.2 Decay form factors in the heavy quark limit

In the heavy quark limit the semileptonic decay of a pseudoscalar meson into  $D^{**}$  is governed by only two form factors [14],  $\tau_{1/2}(w)$  and  $\tau_{3/2}(w)$ , where  $w \equiv v_B \cdot v_{D^{**}} \geq 1$  with  $v_B$  and  $v_{D^{**}}$  denoting the four-velocity of heavy-light meson  $H$  being defined by  $v_H \equiv p_H/m_H$ . Uraltsev has proven the following sum rule [3]:

$$\sum_n \left| \tau_{3/2}^{(n)}(1) \right|^2 - \left| \tau_{1/2}^{(n)}(1) \right|^2 = \frac{1}{4}, \quad (1)$$

where  $\tau_{3/2}^{(n)}(w)$  ( $\tau_{1/2}^{(n)}(w)$ ),  $n = 0, \dots, \infty$  are the form factors for the decay into the  $P_+$  ( $P_-$ ) meson and the tower of its radial excitations<sup>1</sup>.  $w = 1$  corresponds to the zero recoil situation, i.e. the  $B$  and the  $D^{**}$  meson have the same velocity. Eqn. (1) is one of the major among many theoretical arguments in favor of the narrow resonance dominance [1].

Our goal in this paper is to make a direct lattice calculation of  $\tau_{1/2}(1)$  and  $\tau_{3/2}(1)$  using static quarks represented by Wilson lines [15]. However, there is the problem that the  $B \rightarrow D^{**}$  decay amplitude is suppressed at  $w = 1$  due to vanishing kinematical factors, which multiply  $\tau_j(1)$ . This is also a centrifugal barrier effect, i.e. it is impossible to give angular momentum to a meson at rest. Consequently, a computation of the weak current matrix element will trivially give zero. To overcome this difficulty, we use a method, which amounts to compute the operator matrix element based on an expression of the derivative of that matrix element in terms of the recoil four-velocity of the final meson [16, 7]. Thanks to the translational invariance in time of the heavy quark Lagrangian this is then proportional to  $\tau_j(1)(m_{H^j} - m_H)$ ,  $j = 1/2, 3/2$  (cf. eqns. (11) and (12)). The mass splittings  $m_{H^{**}} - m_H$  have already been computed in the static limit with precisely the same setup we are using in this paper [10, 11], i.e. by using  $N_f = 2$  ETMC gauge configurations. We are thus in a position to compute  $\tau_{1/2}(1)$  and  $\tau_{3/2}(1)$  and to confront it with the Uraltsev and other sum rules as well as with other non-perturbative estimates (QCD sum rules, quark models).

Our work should help to clarify the situation in the heavy quark limit. A fair comparison with experiment further needs to estimate the systematic error stemming from the heavy quark limit. After all, the charm quark is not so heavy. The authors of [5, 6] argue that large  $\mathcal{O}(1/m_Q)$  corrections are present. This issue can also be addressed by lattice QCD, but in this work we restrict our computations to the static limit.

The paper is organized as follows. In section 2 we recall the method used to compute  $\tau_{1/2}(1)$  and  $\tau_{3/2}(1)$ . In section 3 we report on the lattice calculation of  $\tau_{1/2}(1)$  and  $\tau_{3/2}(1)$ . In section 4 we perturbatively compute the renormalization constant of the heavy-heavy current and we conclude in section 5.

## 2 Principle of the calculation

To compute the zero-recoil Isgur-Wise functions  $\tau_{1/2}(1)$  and  $\tau_{3/2}(1)$  by means of lattice QCD, we use a method proposed in [7]. We remind it here just for comfort of the reader.

The method consists in using a series of relations derived in ref. [16]. With  $v' = (1, 0, 0, 0)$  and  $v = v' + v_\perp$  denoting the velocities of the ingoing and outgoing mesons, where  $v_\perp$  is spatial up to higher orders in the difference  $v' - v$ , we assume that for some Dirac matrix  $\Gamma_l$

$$\langle H^{**}(v') | \bar{Q}(v') \Gamma_l Q(v) | H^{(*)}(v) \rangle = t_l^m v_{\perp m} \tau_j(w) + \dots \quad (2)$$

Here  $w \equiv v \cdot v'$ ,  $j = 1/2, 3/2$  and  $l, m = 1, 2, 3$  are spatial indices.  $t_l^m$  is a tensor, which depends on the final state ( $H^{**}$ ) and the initial state ( $H^*$  or  $H$ ), and  $Q(v)$  is the static quark field in Heavy Quark Effective Theory. The dots represent higher order terms in  $v' - v$ . From

---

<sup>1</sup>By definition  $\tau_j(w) \equiv \tau_j^{(0)}(w)$ ,  $j = 1/2, 3/2$ .

translational invariance in time direction,

$$\begin{aligned}
& -i\partial_0 \langle H^{**}(v') | \bar{Q}(v') \Gamma_l Q(v) | H^{(*)}(v) \rangle \\
& = -i \langle H^{**}(v') | \bar{Q}(v') \left[ \Gamma_l \vec{D}^0 + \overleftarrow{D}^0 \Gamma_l \right] Q(v) | H^{(*)}(v) \rangle \\
& = t_l^m v_{\perp m} \tau_j(w) \left( m_{H^{**}} - m_H \right) + \dots
\end{aligned} \tag{3}$$

Then we use the field equation  $(v \cdot D)Q(v) = 0$ :

$$D^0 Q(v') = 0 \quad , \quad D^0 Q(v) = -(D \cdot v_{\perp})Q(v), \tag{4}$$

whence from eqn. (3)

$$i \langle H^{**}(v') | \bar{Q}(v') \Gamma_l (D \cdot v_{\perp}) Q(v) | H^{(*)}(v) \rangle = t_l^m v_{\perp m} \tau_j(w) \left( m_{H^{**}} - m_H \right) + \dots, \tag{5}$$

which, in the limit  $v_{\perp} \rightarrow 0$ , converges to the relation

$$i \langle H^{**}(v) | \bar{Q}(v) \Gamma_l D^m Q(v) | H^{(*)}(v) \rangle = t_l^m \tau_j(1) \left( m_{H^{**}} - m_H \right). \tag{6}$$

Applying eqn. (2) to the  $J = 0$   $H_0^*$  state we get from ref. [17]

$$\langle H_0^*(v') | A_i | H(v) \rangle \equiv -\tau_{1/2}(w) v_{\perp i}, \tag{7}$$

where  $A_i$  is the axial current in spatial direction  $i$ , and where the normalization of the states is  $1/\sqrt{2m}$  times the one used in ref. [17]. From eqn. (7) follows

$$\langle H_0^*(v) | A_i D_j | H(v) \rangle = i g_{ij} (m_{H_0^*} - m_H) \tau_{1/2}(1). \tag{8}$$

Analogously for the  $J = 2$   $H_2^*$  state we have

$$\langle H_2^*(v') | A_i | H(v) \rangle \equiv \sqrt{3} \tau_{3/2}(w) \epsilon_i^{*j} v_{\perp j} + \dots, \tag{9}$$

where  $\epsilon_i^{*j}$  is the polarization tensor, whence

$$\langle H_2^*(v) | A_i D_j | H(v) \rangle = -i\sqrt{3} \left( m_{H_2^*} - m_H \right) \tau_{3/2}(1) \epsilon_{ij}^*. \tag{10}$$

Finally  $\tau_{1/2}(1)$  and  $\tau_{3/2}(1)$  can be obtained from the following matrix elements:

$$\tau_{1/2}(1) = \left| \frac{\langle H_0^* | \bar{Q} \gamma_5 \gamma_z D_z Q | H \rangle}{m_{H_0^*} - m_H} \right| \tag{11}$$

$$\tau_{3/2}(1) = \left| \frac{\langle H_2^* | \bar{Q} \gamma_5 (\gamma_x D_x - \gamma_y D_y) Q | H \rangle}{\sqrt{6} (m_{H_2^*} - m_H)} \right|. \tag{12}$$

There is no mixing of the operators  $A_i D_j$  with dimension 3 (hence linearly divergent) heavy-heavy operators to be feared on the lattice: indeed we are interested in a parity-changing transition and all dimension 3 operators have vanishing matrix elements between positive and negative parity states<sup>2</sup>. There are no logarithmic divergence either thanks to the vanishing of the vector and axial currents’ anomalous dimension in HQET at zero recoil. By consequence there is no conceptual issue concerning the extrapolation to the continuum limit of such a calculation. It needs only a finite renormalization constant to match the lattice result with a continuum-like scheme value, as we will discuss in Section 4.

### 3 Lattice computation of $\tau_{1/2}$ and $\tau_{3/2}$ at zero recoil

#### 3.1 Simulation setup

We use  $N_f = 2$  flavor  $24^3 \times 48$  Wilson twisted mass gauge configurations produced by the European Twisted Mass Collaboration (ETMC). Here we only give a brief summary of the setup, which is explained in detail in [18, 19, 20].

The gauge action is tree-level Symanzik improved [21] with  $\beta = 3.9$  corresponding to a lattice spacing  $a = 0.0855(5)$  fm:

$$S_G[U] = \frac{\beta}{6} \left( b_0 \sum_{x, \mu \neq \nu} \text{Tr} \left( 1 - P^{1 \times 1}(x; \mu, \nu) \right) + b_1 \sum_{x, \mu \neq \nu} \text{Tr} \left( 1 - P^{1 \times 2}(x; \mu, \nu) \right) \right), \quad (13)$$

where  $b_0 = 1 - 8b_1$  and  $b_1 = -1/12$ .

The fermionic action is Wilson twisted mass with two degenerate flavors [22, 23, 24]:

$$S_F[\chi, \bar{\chi}, U] = a^4 \sum_x \bar{\chi}(x) \left( D_W + i\mu_q \gamma_5 \tau_3 \right) \chi(x), \quad (14)$$

where

$$D_W = \frac{1}{2} \left( \gamma_\mu \left( \nabla_\mu + \nabla_\mu^* \right) - a \nabla_\mu^* \nabla_\mu \right) + m_0, \quad (15)$$

$\nabla_\mu$  and  $\nabla_\mu^*$  are the standard gauge covariant forward and backward derivatives,  $m_0$  and  $\mu_q$  are the bare untwisted and twisted quark masses and  $\chi = (\chi^{(u)}, \chi^{(d)})$  are the fermionic fields in the twisted basis.

We consider three different values of the light quark mass, which amount to “pion masses” in the range  $300 \text{ MeV} \lesssim m_{\text{PS}} \lesssim 450 \text{ MeV}$  (cf. Table 1).  $m_0$  has been tuned to its critical value at the lightest  $\mu_q$  value, i.e. at  $\mu_q = 0.0040$ .

---

<sup>2</sup>Of course the situation is different by instance for the matrix element  $\langle H | \bar{h} \mathbf{D}^2 h | H \rangle$ , related to the HQET parameter  $\lambda_1$  or the kinetic momentum  $\mu_\pi^2$  for which a subtraction is necessary to its computation on the lattice [8, 9].

| $\mu_q$ | $m_{\text{PS}}$ in MeV | number of gauge configurations |
|---------|------------------------|--------------------------------|
| 0.0040  | 314(2)                 | 1400                           |
| 0.0064  | 391(1)                 | 1450                           |
| 0.0085  | 448(1)                 | 1350                           |

Table 1: twisted quark masses  $\mu_q$ , pion masses  $m_{\text{PS}}$  and number of gauge configurations.

### 3.2 Static and light quark propagators

The propagator of a static quark is essentially a Wilson line in time direction:

$$\langle Q(x)\bar{Q}(y) \rangle_{Q,\bar{Q}} = \delta^{(3)}(\mathbf{x} - \mathbf{y})U^{(\text{HYP2})}(x; y) \left( \Theta(y_0 - x_0)\frac{1 - \gamma_0}{2} + \Theta(x_0 - y_0)\frac{1 + \gamma_0}{2} \right), \quad (16)$$

where  $\langle \dots \rangle_{Q,\bar{Q}}$  denotes the integration over the static quark field and  $U(x; y)$  is a path ordered product of links along the straight path from  $x$  to  $y$ . To improve the signal-to-noise ratio we use the HYP2 static action [25, 26, 27].

For the light quarks we use four stochastic spin diluted timeslice propagators ( $\mathcal{Z}_2 \times \mathcal{Z}_2$  sources with randomly chosen components  $\pm 1 \pm i$ ) for each gauge configuration. For details we refer to [11], where exactly the same setup has been used.

### 3.3 Static-light meson creation operators

In the static limit there are no interactions involving the heavy quark spin. Therefore, it is convenient to classify static-light mesons according to  $j^{\mathcal{P}}$ , where  $j$  denotes the angular momentum of the light degrees of freedom and  $\mathcal{P}$  parity. In particular we are interested in the sectors  $j^{\mathcal{P}} = (1/2)^-$ ,  $j^{\mathcal{P}} = (1/2)^+$  and  $j^{\mathcal{P}} = (3/2)^+$ . We label the corresponding static-light mesons, i.e. the ground states in these angular momentum/parity sectors, by  $S$ ,  $P_-$  and  $P_+$  respectively.

To create such static-light mesons on the lattice we use operators

$$\mathcal{O}^{(\Gamma)}(\mathbf{x}) = \bar{Q}(\mathbf{x}) \sum_{\mathbf{n}=\pm\hat{\mathbf{e}}_1,\pm\hat{\mathbf{e}}_2,\pm\hat{\mathbf{e}}_3} \Gamma(\hat{\mathbf{n}})U(\mathbf{x}; \mathbf{x} + \mathbf{r}\mathbf{n})\chi^{(u)}(\mathbf{x} + \mathbf{r}\mathbf{n}), \quad (17)$$

where  $\bar{Q}$  creates a static antiquark at position  $\mathbf{x}$ ,  $\chi^{(u)}$  creates a light quark in the twisted basis at position  $\mathbf{x} + \mathbf{r}\mathbf{n}$ ,  $U$  is a product of spatial links along the straight path between  $\mathbf{x}$  and  $\mathbf{x} + \mathbf{r}\mathbf{n}$ , and  $\Gamma$  is a combination of spherical harmonics and  $\gamma$  matrices yielding a well defined behavior under cubic rotations (cf. Table 2).

To optimize the ground state overlap of these static-light meson states, we use Gaussian smearing [28] for light quark operators and APE smearing [29] for spatial links (parameters  $\kappa_{\text{Gauss}} = 0.5$ ,  $N_{\text{Gauss}} = 30$ ,  $\alpha_{\text{APE}} = 0.5$ ,  $N_{\text{APE}} = 10$  and  $r = 3$  as in [11]).

| $\Gamma(\hat{\mathbf{n}})$                                       | $O_h$ | $j$               |
|--|-------|-------------------|
| $\gamma_5$   | $A_1$ | $1/2, 7/2, \dots$ |
| $1$  |       | $1/2, 7/2, \dots$ |
| $\gamma_x \hat{n}_x - \gamma_y \hat{n}_y$ (and cyclic)           | $E$   | $3/2, 5/2, \dots$ |
| $\gamma_5(\gamma_x \hat{n}_x - \gamma_y \hat{n}_y)$ (and cyclic) |       | $3/2, 5/2, \dots$ |

Table 2: static-light meson creation operators.

### 3.4 Static-light meson masses

Since we work in the twisted basis, where each of the operators listed in Table 2 creates both  $\mathcal{P} = +$  and  $\mathcal{P} = -$  states, it is convenient to determine  $\mathcal{P} = +$  and  $\mathcal{P} = -$  static-light meson masses from the same correlation matrix.

For  $S$  and  $P_-$  we compute the  $2 \times 2$  matrix

$$\mathcal{C}_{JK}(t) = \left\langle \left( \mathcal{O}^{(\Gamma_J)}(t) \right)^\dagger \mathcal{O}^{(\Gamma_K)}(0) \right\rangle, \quad (18)$$

where  $\Gamma_J \in \{\gamma_5, 1\}$ , and solve the generalized eigenvalue problem

$$\mathcal{C}_{JK}(t)v_K^{(n)}(t) = \mathcal{C}_{JK}(t_0)v_K^{(n)}(t_0)\lambda^{(n)}(t, t_0) \quad , \quad t_0 = 1 \quad (19)$$

(cf. [30, 31]). The meson masses  $m(S)$  and  $m(P_-)$  are determined by performing  $\chi^2$  minimizing fits to effective mass plateaus,

$$m_{\text{effective}}^{(n)}(t) = \ln \left( \frac{\lambda^{(n)}(t, t_0)}{\lambda^{(n)}(t+1, t_0)} \right), \quad (20)$$

at large temporal separations  $t$  (as indicated in Figure 1 our fitting range is  $6 \leq t \leq 11$ ). The parity of the corresponding states, i.e. whether it is  $S$  or  $P_-$ , can be extracted from the eigenvectors  $v_J^{(n)}$  (for a detailed discussion, of how to identify parity, cf. [11]). Results of meson masses and mass differences and corresponding reduced  $\chi^2$  values are listed in Table 3.

For  $m(P_+)$  we proceed analogously this time computing the  $2 \times 2$  matrix (19), where  $\Gamma_J \in \{\gamma_x \hat{n}_x - \gamma_y \hat{n}_y, \gamma_5(\gamma_x \hat{n}_x - \gamma_y \hat{n}_y)\}$ .

By solving the generalized eigenvalue problem (19) we have also obtained appropriate linear combinations of twisted basis meson creation operators with well defined parity. To be more precise the operators

$$\mathcal{O}^{(S)} = v_{\gamma_5}^{(S)}(t)\mathcal{O}^{(\gamma_5)} + v_1^{(S)}(t)\mathcal{O}^{(1)} \quad (21)$$

$$\mathcal{O}^{(P_-)} = v_{\gamma_5}^{(P_-)}(t)\mathcal{O}^{(\gamma_5)} + v_1^{(P_-)}(t)\mathcal{O}^{(1)} \quad (22)$$

$$\mathcal{O}^{(P_+)} = v_{\gamma_x \hat{n}_x - \gamma_y \hat{n}_y}^{(P_+)}(t)\mathcal{O}^{(\gamma_x \hat{n}_x - \gamma_y \hat{n}_y)} + v_{\gamma_5(\gamma_x \hat{n}_x - \gamma_y \hat{n}_y)}^{(P_+)}(t)\mathcal{O}^{(\gamma_5(\gamma_x \hat{n}_x - \gamma_y \hat{n}_y))} \quad (23)$$

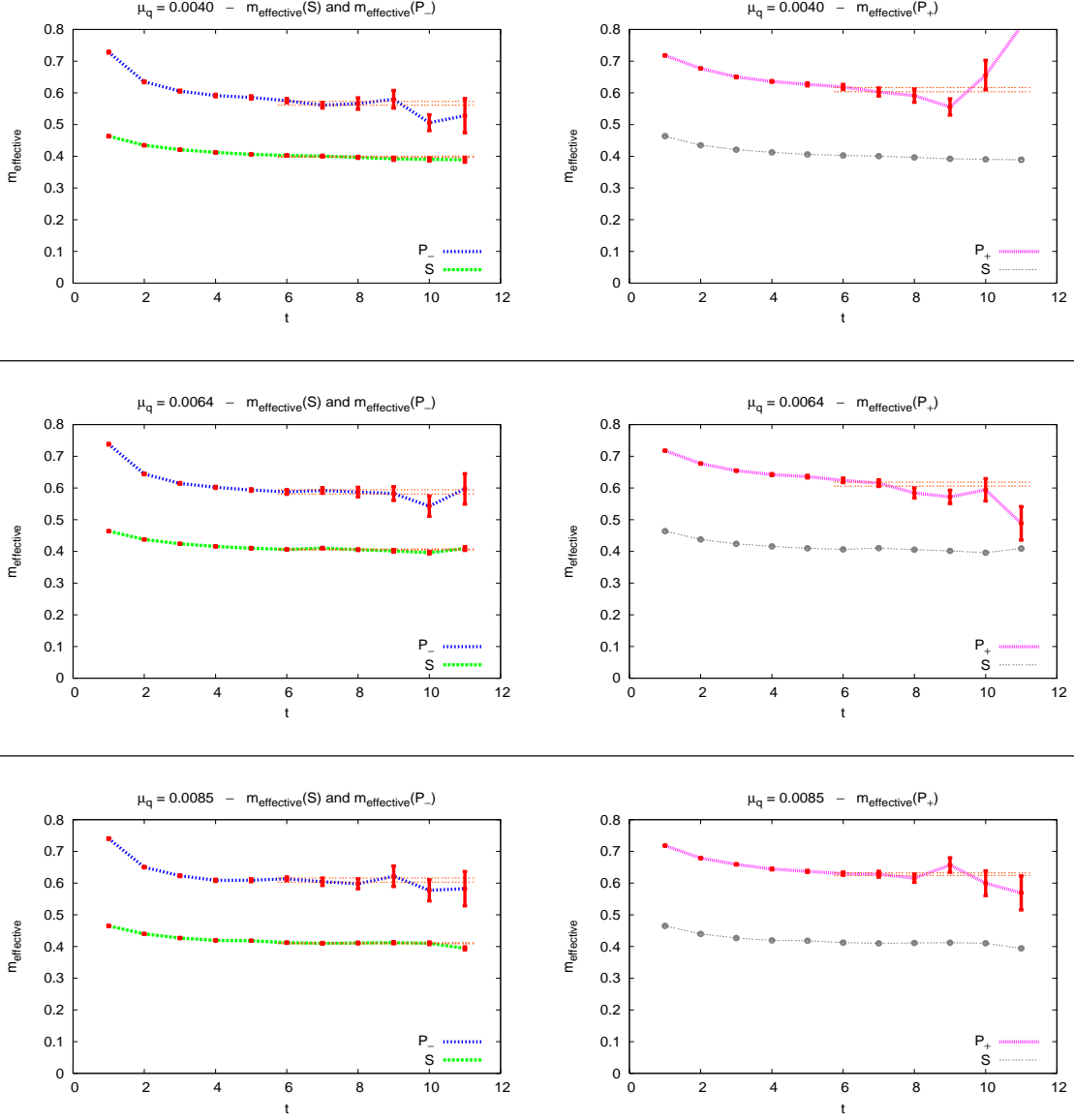


Figure 1: effective masses for  $S$ ,  $P_-$  and  $P_+$  for  $\mu_q \in \{0.0040, 0.0064, 0.0085\}$ .

create static-light meson states, which have the same quantum numbers  $j^P$  as the states of interest,  $|S\rangle$ ,  $|P_- \rangle$  and  $|P_+ \rangle$  respectively. Since the  $t$  dependence of the eigenvectors  $v_j^{(n)}$  is very weak [32], results are essentially unaffected by the choice of  $t$  (we have used  $t = 6$  for all results presented in the following).



| $\mu_q$ | $m(S)$     | $\chi^2/\text{dof}$ | $m(P_-)$   | $\chi^2/\text{dof}$ | $m(P_+)$   | $\chi^2/\text{dof}$ |
|---------|------------|---------------------|------------|---------------------|------------|---------------------|
| 0.0040  | 0.3987(19) | 1.79                | 0.5670(60) | 1.69                | 0.6101(66) | 2.46                |
| 0.0064  | 0.4061(17) | 1.93                | 0.5877(67) | 0.45                | 0.6121(64) | 3.01                |
| 0.0085  | 0.4104(17) | 2.23                | 0.6095(65) | 0.49                | 0.6283(41) | 0.87                |

| $\mu_q$ | $m(P_-) - m(S)$ | $m(P_+) - m(S)$ |
|---------|-----------------|-----------------|
| 0.0040  | 0.1683(65)      | 0.2114(62)      |
| 0.0064  | 0.1817(69)      | 0.2060(63)      |
| 0.0085  | 0.1991(63)      | 0.2179(41)      |

Table 3: static-light meson masses and mass differences for  $\mu_q \in \{0.0040, 0.0064, 0.0085\}$ .

### 3.5 Two-point functions and their ground state norms

After having obtained the linear combinations of twisted basis operators (21) to (23) the two-point functions

$$\langle (\mathcal{O}^{(S)}(t))^\dagger \mathcal{O}^{(S)}(0) \rangle, \quad \langle (\mathcal{O}^{(P_-)}(t))^\dagger \mathcal{O}^{(P_-)}(0) \rangle, \quad \langle (\mathcal{O}^{(P_+)}(t))^\dagger \mathcal{O}^{(P_+)}(0) \rangle \quad (24)$$

are straightforward to compute.

From these two-point functions we also determine the ground state norms of the corresponding  $j^P$  sectors,  $N(S)$ ,  $N(P_-)$  and  $N(P_+)$ , by fitting exponentials at large temporal separations. To be more precise, we obtain e.g.  $N(S)$  by fitting  $N(S)^2 e^{-mt}$  to  $\langle (\mathcal{O}^{(S)}(t))^\dagger \mathcal{O}^{(S)}(0) \rangle$  with  $N(S)$  and  $m$  as degrees of freedom. Results and corresponding reduced  $\chi^2$  values are listed in Table 4 (fitting range  $6 \leq t \leq 12$ ).

| $\mu_q$ | $N(S)$     | $\chi^2/\text{dof}$ | $N(P_-)$    | $\chi^2/\text{dof}$ | $N(P_+)$   | $\chi^2/\text{dof}$ |
|---------|------------|---------------------|-------------|---------------------|------------|---------------------|
| 0.0040  | 0.3271(26) | 0.21                | 0.2998(93)  | 0.33                | 0.1139(26) | 1.43                |
| 0.0064  | 0.3358(20) | 0.23                | 0.3074(87)  | 0.13                | 0.1120(27) | 1.68                |
| 0.0085  | 0.3397(22) | 0.22                | 0.3139(103) | 0.08                | 0.1212(22) | 0.28                |

Table 4: ground state norms for  $\mu_q \in \{0.0040, 0.0064, 0.0085\}$ .

### 3.6 Three-point functions and form factors $\tau_{1/2}$ and $\tau_{3/2}$

In analogy to effective masses we define effective form factors

$$\begin{aligned} & \tau_{1/2, \text{effective}}(t_0 - t_1, t_1 - t_2) \\ &= \frac{1}{Z_{\mathcal{D}}} \left| \frac{N(P_-) N(S) \langle (\mathcal{O}^{(P_-)}(t_0))^\dagger (\bar{Q} \gamma_5 \gamma_z D_z Q)(t_1) \mathcal{O}^{(S)}(t_2) \rangle}{(m(P_-) - m(S)) \langle (\mathcal{O}^{(P_-)}(t_0))^\dagger \mathcal{O}^{(P_-)}(t_1) \rangle \langle (\mathcal{O}^{(S)}(t_1))^\dagger \mathcal{O}^{(S)}(t_2) \rangle} \right| \end{aligned} \quad (25)$$

$$\begin{aligned} & \tau_{3/2,\text{effective}}(t_0 - t_1, t_1 - t_2) \\ &= \frac{1}{Z_{\mathcal{D}}} \left| \frac{N(P_+) N(S) \langle (\mathcal{O}^{(P_+)}(t_0))^\dagger (\bar{Q}\gamma_5(\gamma_x D_x - \gamma_y D_y)Q)(t_1) \mathcal{O}^{(S)}(t_2) \rangle}{\sqrt{6} (m(P_+) - m(S)) \langle (\mathcal{O}^{(P_+)}(t_0))^\dagger \mathcal{O}^{(P_+)}(t_1) \rangle \langle (\mathcal{O}^{(S)}(t_1))^\dagger \mathcal{O}^{(S)}(t_2) \rangle} \right| \end{aligned} \quad (26)$$

( $Z_{\mathcal{D}} = 0.976$  is a lattice renormalization constant, which we derive and discuss in detail in section 4). These effective form factors are related to  $\tau_{1/2}$  and  $\tau_{3/2}$  via (11) and (12):

$$\tau_{1/2}(1) = \lim_{t_0-t_1 \rightarrow \infty, t_1-t_2 \rightarrow \infty} \tau_{1/2,\text{effective}}(t_0 - t_1, t_1 - t_2) \quad (27)$$

$$\tau_{3/2}(1) = \lim_{t_0-t_1 \rightarrow \infty, t_1-t_2 \rightarrow \infty} \tau_{3/2,\text{effective}}(t_0 - t_1, t_1 - t_2). \quad (28)$$

Computation of the three-point functions appearing in (25) and (26) is again straightforward. We chose to represent the covariant derivative acting on the static quark field symmetrically by

$$D_j Q(\mathbf{x}, t) = \frac{1}{2} \left( U_j(\mathbf{x}, t) Q(\mathbf{x} + \mathbf{e}_j, t) - \left( U_j(\mathbf{x} - \mathbf{e}_j, t) \right)^\dagger Q(\mathbf{x} - \mathbf{e}_j, t) \right). \quad (29)$$

To optimally exploit our gauge configurations and propagator inversions, we average over all three-point functions, which are related by the lattice symmetries  $\gamma_5$  hermiticity, parity, time reversal, charge conjugation and cubic rotations.

The resulting effective form factors  $\tau_{1/2,\text{effective}}(t_0 - t_1, t_1 - t_2)$  and  $\tau_{3/2,\text{effective}}(t_0 - t_1, t_1 - t_2)$  are shown in Figure 2 as functions of  $t_0 - t_1$  for fixed  $t_0 - t_2 \in \{10, 12\}$ . Within statistical errors these effective form factors exhibit plateaus for  $t_0 - t_1 \approx (t_0 - t_2)/2$ , i.e. when both temporal separations,  $t_0 - t_1$  and  $t_1 - t_2$ , are large. We determine  $\tau_{1/2}$  and  $\tau_{3/2}$  by performing  $\chi^2$  minimizing fits to the central three data points as indicated in Figure 2. Results for  $t_0 - t_2 = 10$  and for  $t_0 - t_2 = 12$ , which are listed in Table 5, are in agreement within statistical errors. We consider this a strong indication that contributions from excited states at these temporal separations are essentially negligible and that the plateaus of the effective form factors indeed correspond to  $\tau_{1/2}$  and  $\tau_{3/2}$ . In the following discussions we only quote the numbers corresponding to  $t_0 - t_2 = 10$ , since their statistical errors are significantly smaller than those for  $t_0 - t_2 = 12$ .

| $\mu_q$ | $t_0 - t_2$ | $\tau_{1/2}$ | $\tau_{3/2}$ | $\tau_{3/2}/\tau_{1/2}$ | $(\tau_{3/2})^2 - (\tau_{1/2})^2$ |
|---------|-------------|--------------|--------------|-------------------------|-----------------------------------|
| 0.0040  | 10          | 0.299(14)    | 0.519(13)    | 1.74(9)                 | 0.180(16)                         |
|         | 12          | 0.267(26)    | 0.536(25)    | 2.01(21)                | 0.216(30)                         |
| 0.0064  | 10          | 0.312(10)    | 0.538(13)    | 1.73(6)                 | 0.193(13)                         |
|         | 12          | 0.278(19)    | 0.549(21)    | 1.98(14)                | 0.225(23)                         |
| 0.0085  | 10          | 0.308(12)    | 0.522(8)     | 1.69(6)                 | 0.177(9)                          |
|         | 12          | 0.287(24)    | 0.544(14)    | 1.90(17)                | 0.214(21)                         |

Table 5:  $\tau_{1/2}$  and  $\tau_{3/2}$  for  $t_0 - t_2 \in \{10, 12\}$  and  $\mu_q \in \{0.0040, 0.0064, 0.0085\}$ .

As expected from operator product expansion,  $\tau_{3/2}(1)$  is significantly larger than  $\tau_{1/2}(1)$ . More-

over the Uraltsev sum rule [3],

$$\sum_n \left| \tau_{3/2}^{(n)}(1) \right|^2 - \left| \tau_{1/2}^{(n)}(1) \right|^2 = \frac{1}{4}, \quad (30)$$

is almost fulfilled by the ground state contributions  $\tau_{1/2}^{(0)}(1) \equiv \tau_{1/2}(1)$  and  $\tau_{3/2}^{(0)}(1) \equiv \tau_{3/2}(1)$ .

Finally we use our results at three different light quark masses (cf. Table 1) to perform a linear extrapolation of the form factors in  $(m_{\text{PS}})^2$  to the physical  $u/d$  quark mass ( $m_{\text{PS}} = 135 \text{ MeV}$ ).

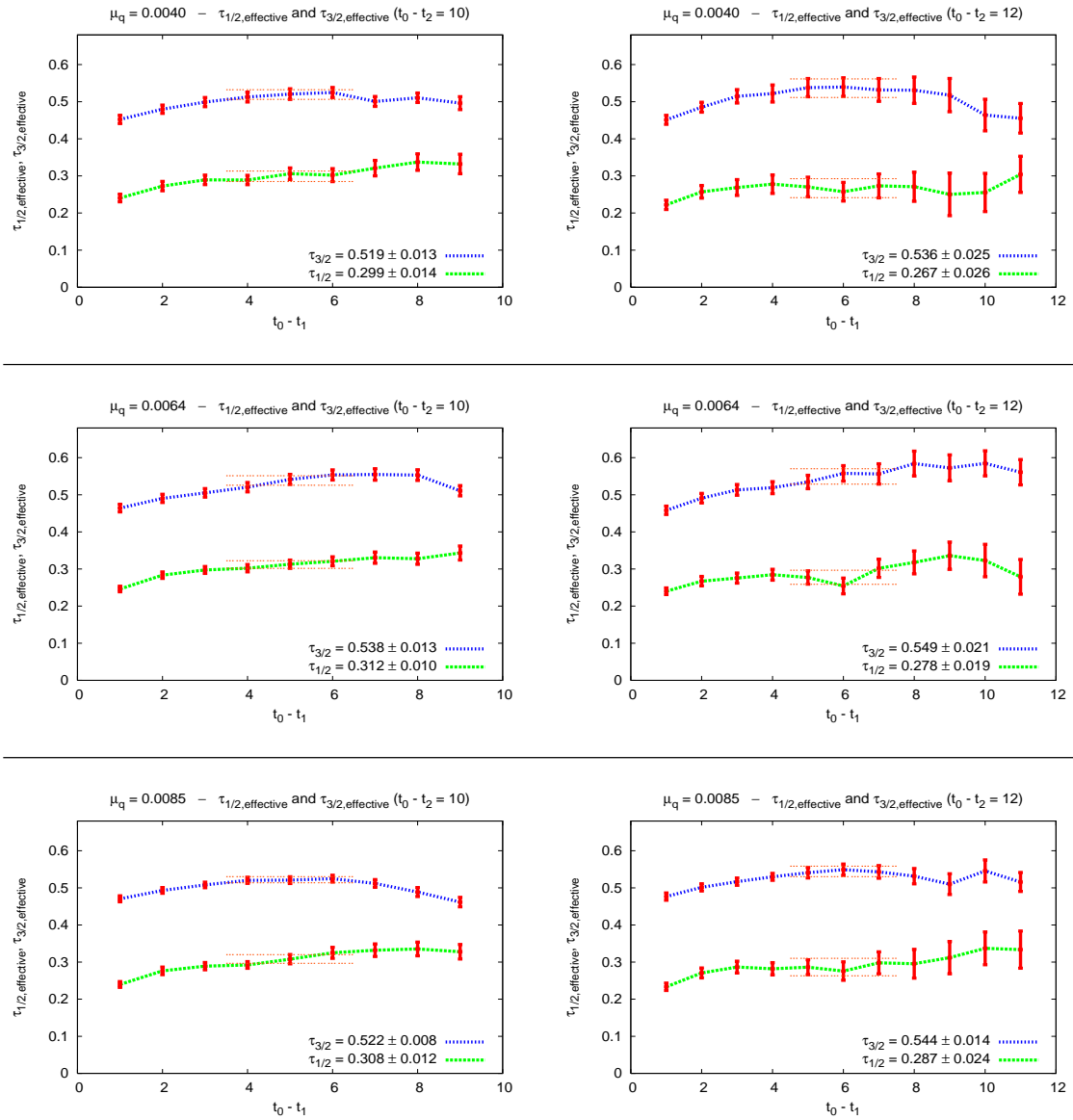


Figure 2: effective form factors  $\tau_{1/2,\text{effective}}$  and  $\tau_{3/2,\text{effective}}$  for  $t_0 - t_2 \in \{10, 12\}$  and  $\mu_q \in \{0.0040, 0.0064, 0.0085\}$ .

Results are shown in Figure 3 and Table 6. The qualitative picture for  $u/d$  quark masses is the same as for the heavier masses used directly in our simulations:  $\tau_{3/2}^{m_{\text{phys}}}(1) = 0.526(23)$  is significantly larger than  $\tau_{1/2}^{m_{\text{phys}}}(1) = 0.296(26)$  supporting the “theory expectation” that a decay of a  $B$  meson to a  $j = 3/2$   $P$  wave  $D$  meson is more likely than to a  $j = 1/2$   $P$  wave  $D$  meson.

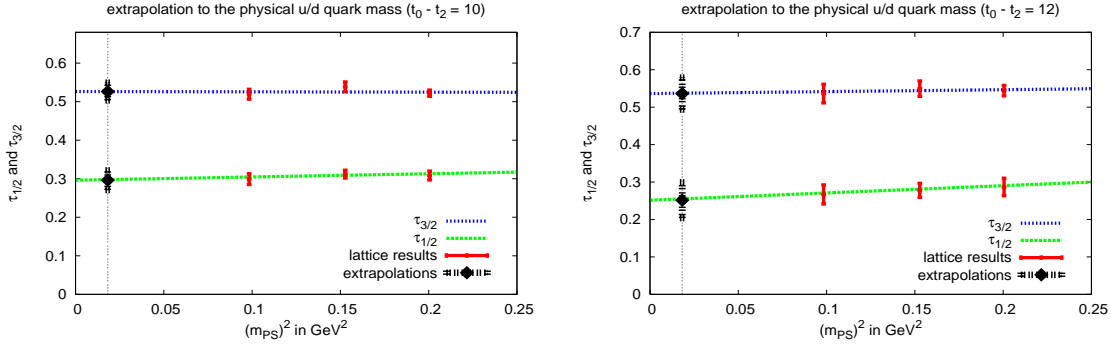


Figure 3: linear extrapolation of  $\tau_{1/2}$  and  $\tau_{3/2}$  to the  $u/d$  quark mass for  $t_0 - t_2 \in \{10, 12\}$ .

| $t_0 - t_2$ | $\tau_{1/2}(1)$ | $\chi^2/\text{dof}$ | $\tau_{3/2}(1)$ | $\chi^2/\text{dof}$ |
|-------------|-----------------|---------------------|-----------------|---------------------|
| 10          | 0.296(26)       | 0.34                | 0.526(23)       | 1.43                |
| 12          | 0.251(48)       | 0.00                | 0.536(43)       | 0.12                |

Table 6: linear extrapolation of  $\tau_{1/2}$  and  $\tau_{3/2}$  to the  $u/d$  quark mass for  $t_0 - t_2 \in \{10, 12\}$ .

## 4 Perturbative renormalization of the static current $\bar{Q}\gamma_5\gamma_i D_j Q$

In this section we derive the analytical formulae and give the numerical values of the renormalization constant  $Z_D$  of the dimension 4 current  $O_{ij} = \bar{Q}\gamma_5\gamma_i D_j Q$  computed at first order of perturbation theory for the HYP smeared static quark action and both the standard Wilson plaquette and the tree-level Symanzik improved gauge action.

### 4.1 Definitions

The bare propagator of a static quark on the lattice is

$$\begin{aligned}
 S^B(p) &= \frac{a}{1 - e^{-ip_4 a} + a\delta m + a\Sigma(p)} = \frac{a}{1 - e^{-ip_4 a}} \sum_n \left( -\frac{a(\delta m + \Sigma(p))}{1 - e^{-ip_4 a}} \right)^n \\
 &\equiv Z_{2h} S^R(p).
 \end{aligned} \tag{31}$$

Choosing the renormalization conditions

$$(S^R)^{-1}(p) \Big|_{ip_4 \rightarrow 0} = ip_4 \quad , \quad \delta m = -\Sigma(p_4 = 0) \tag{32}$$

implies

$$Z_{2h} = 1 - \frac{d\Sigma}{d(ip_4)} \Big|_{ip_4 \rightarrow 0}. \quad (33)$$

The bare vertex function  $V_{ij}^B(p)$  is defined as

$$\begin{aligned} V_{ij}^B(p) &= (S^B)^{-1}(p) \sum_{x,y} e^{ip(x-y)} \langle Q^B(x) O_{ij}^B(0) \bar{Q}^B(y) \rangle (S^B)^{-1}(p) \\ &= \frac{Z_{\mathcal{D}}}{Z_{2h}} (S^R)^{-1}(p) \sum_{x,y} e^{ip(x-y)} \langle Q^R(x) O_{ij}^R(0) \bar{Q}^R(y) \rangle (S^R)^{-1}(p), \end{aligned} \quad (34)$$

where

$$O_{ij}^B(0) = Z_{\mathcal{D}} O_{ij}^R(0). \quad (35)$$

$V_{ij}^B(p)$  can be written as

$$V_{ij}^B(p) = (1 + \delta V) \bar{u}(p) \gamma_i \gamma_5 p_j u(p) \equiv (1 + \delta V) V_{ij}^R(p). \quad (36)$$

$\delta V$  is given by all the 1PI one-loop diagrams containing the vertex.

## 4.2 Analytical formulae and results

The notations used in this section and the Feynman rules are listed in appendix A. They are the same as in [33] except for the gluon propagator having the form

$$D_{\mu\nu} = C_0^{-1} D_{\mu\nu}^{\text{plaq}} + \Delta_{\mu\nu} \quad (37)$$

[34], where  $C_0 = c_0 + 8c_1 + 16c_2 + 8c_3 \equiv 1$ ,  $c_1 = -1/12$ ,  $c_2 = c_3 = 0$  for the case of the tree-level Symanzik improved gauge action and

$$\Delta_{\mu\nu} = \delta_{\mu\nu} K_\mu + 4L_{\mu\nu} N_\mu N_\nu. \quad (38)$$

Finally  $K_\mu$  and  $L_{\mu\nu}$  are complicated expressions, which do not need to be reproduced here. The only relevant features for this work are that  $\Delta_{\mu\nu}$  is regular in the infrared regime and  $K_\mu = K^0 + 4N_\mu^2 K'_\mu$ .

The static quark self-energy expressed at the first order of perturbation theory is given by  $\Sigma(p) = -(F_1 + F_2)$ , where  $F_1$  and  $F_2$  correspond to the diagrams shown in Figure 4(a) and (b):

$$F_1 = -\frac{4}{3a} g_0^2 \int_k h_{4i} h_{4j} D_{ij} \frac{e^{-i(k_4 + 2ap_4)}}{1 - e^{-i(k_4 + ap_4)} + \epsilon} = F_1^{\text{plaq}} + F'_1 \quad (39)$$

$$\begin{aligned}
F_1^{\text{plaq}} &= -\frac{4}{3a}g_0^2 \int_k \frac{D_4^2 + \sum_{i=1}^3 G_{4i}^2}{2W + a^2\lambda^2} \frac{e^{-i(k_4+2ap_4)}}{1 - e^{-i(k_4+ap_4)} + \epsilon} \\
&=_{ap_4 \rightarrow 0} \frac{4}{3a}g_0^2 \int_{\vec{k}} \frac{D_4^2(-iE) + \sum_{i=1}^3 G_{4i}^2(-iE)}{4E\sqrt{1+E^2}} \frac{1}{1 - e^{E'}} \\
&\quad + \frac{4}{3}g_0^2 ip_4 \int_{\vec{k}} \frac{D_4^2(-iE) + \sum_{i=1}^3 G_{4i}^2(-iE)}{2E\sqrt{1+E^2}} \left[ \frac{1}{e^{E'} - 1} + \frac{1}{2} \frac{1}{(e^{E'} - 1)^2} \right]
\end{aligned} \tag{40}$$

$$\begin{aligned}
F_1' &= -\frac{4}{3a}g_0^2 \int_k h_{4i}h_{4j}\Delta_{ij} \frac{e^{-i(k_4+2ap_4)}}{1 - e^{-i(k_4+ap_4)} + \epsilon} = \\
&=_{ap_4 \rightarrow 0} -\frac{4}{3a}g_0^2 \int_k \frac{M_4 - iN_4}{2iN_4 + \epsilon M_4} \left( D_4^2 K^0 + N_4^2 \Lambda \right) \\
&\quad + \frac{8}{3}g_0^2 ip_4 \int_k \left[ \frac{M_4 - iN_4}{2iN_4 + \epsilon M_4} + \frac{1}{2} \left( \frac{M_4 - iN_4}{2iN_4 + \epsilon M_4} \right)^2 \right] \left( D_4^2 K^0 + N_4^2 \Lambda \right) \\
&= \frac{2}{3a}g_0^2 \int_k \left( D_4^2 K^0 + N_4^2 \Lambda \right) - \frac{1}{3}g_0^2 ip_4 \int_k \left[ M_4^2 \Lambda + 3 \left( D_4^2 K^0 + N_4^2 \Lambda \right) \right]
\end{aligned} \tag{41}$$

$$\begin{aligned}
N_4^2 \Lambda &= 4 \left( D_4^2 N_4^2 (K_4' + L_{44}) + \frac{1}{4} \sum_i G_{4i}^2 (K^0 + 4N_i^2 K_i') + 2D_4 N_4 \sum_{i=1}^3 G_{4i} N_i L_{4i} \right. \\
&\quad \left. + 2 \sum_{i,j=1}^3 G_{4i} G_{4j} N_i N_j L_{ij} \right)
\end{aligned} \tag{42}$$

$$F_2 = -\frac{1}{2} \frac{4g_0^2}{3a} e^{-iap_4} \int_k h_{4i}h_{4j} D_{ij} = F_2^{\text{plaq}} + F_2' \tag{43}$$

$$\begin{aligned}
F_2^{\text{plaq}} &= -\frac{1}{2} \frac{4g_0^2}{3a} e^{-iap_4} \int_k \frac{D_4^2 + \sum_{i=1}^3 G_{4i}^2}{2W} \\
&=_{ap_4 \rightarrow 0} -\frac{1}{2} \frac{4g_0^2}{3} \left( 1/a - ip_4 \right) \int_k \frac{D_4^2 + \sum_{i=1}^3 G_{4i}^2}{2W}
\end{aligned} \tag{44}$$

$$F_2' = -\frac{1}{2} \frac{4g_0^2}{3a} e^{-iap_4} \int_k h_{4i}h_{4j}\Delta_{ij} =_{ap_4 \rightarrow 0} -\frac{1}{2} \frac{4g_0^2}{3} \left( 1/a - ip_4 \right) \int_k \left( D_4^2 K^0 + N_4^2 \Lambda \right). \tag{45}$$



Figure 4: self-energy corrections.

The factor 1/2 has been introduced to compensate the over-counting of the factor 2 in the Feynman rule of the two-gluon vertex, when a closed gluonic loop is computed.

The other terms entering the above integrals cancel, because the contour can be closed in the complex plane without including the pole  $k_4 = -p_4 + i \ln(1 + \epsilon)$ . Finally we can write

$$F_1 \equiv -\frac{g_0^2}{12\pi^2} \left[ \left( f_1^{\text{plaq}}(\alpha_i) + f_1'(\alpha_i, c_i) \right) / a + ip_4 \left( 2 \ln(a^2 \lambda^2) + f_2^{\text{plaq}}(\alpha_i) + f_2'(\alpha_i, c_i) \right) \right] \quad (46)$$

$$F_2 \equiv -\frac{g_0^2}{12\pi^2} \left( 1/a - ip_4 \right) \left( f_3^{\text{plaq}}(\alpha_i) + f_3'(\alpha_i, c_i) \right). \quad (47)$$

The linearly divergent part in  $1/a$  of the self-energy is given by

$$\Sigma_0(\alpha_i) = \frac{g_0^2}{12\pi^2 a} \sigma_0(\alpha_i) \quad , \quad \sigma_0 = f_1 + f_1' + f_3 + f_3', \quad (48)$$

while the wave function renormalization  $Z_{2h}$  reads

$$Z_{2h}(\alpha_i) = 1 + \frac{g_0^2}{12\pi^2} \left( -2 \ln(a^2 \lambda^2) + z_2(\alpha_i) \right) \quad , \quad z_2 = f_3 + f_3' - (f_2 + f_2'). \quad (49)$$

In Table 7 we have collected the numerical values of  $f_i$ ,  $f_i'$ ,  $\sigma_0$  and  $z_2$  for different kinds of static quark and gluonic actions.

The vertex function  $V_{ij}^B$  is obtained by writing

$$V_{ij}^B = V_{ij}^0 + V_{ij}^1 + V_{ij}^2 \quad , \quad V_{ij}^k(\alpha_i) = \bar{u}(p) \gamma_i \gamma^5 u(p) V_j^k(\alpha_i) \quad , \quad l = 0, 1, 2 \quad (50)$$

corresponding to the diagrams (a), (b) and (c) in Figure 5. The contribution  $V_{ij}^0$  is given by computing

$$V_j^0(\alpha_i) = -\frac{4i}{3a} g_0^2 \int_k h_{4k} h_{4l} D_{kl} \sin(k + ap)_j \frac{e^{-i(k_4 + 2ap_4)}}{(1 - e^{-i(k_4 + ap_4)} + \epsilon)^2} = V_j^{0,\text{plaq}} + V_j'^0 \quad (51)$$

$$V_j^{0,\text{plaq}} = -\frac{4i}{3a} g_0^2 \int_k \frac{D_4^2 + \sum_{i=1}^3 G_{4i}^2}{2W + a^2 \lambda^2} \sin(k + ap)_j \frac{e^{-i(k_4 + 2ap_4)}}{(1 - e^{-i(k_4 + ap_4)} + \epsilon)^2}$$

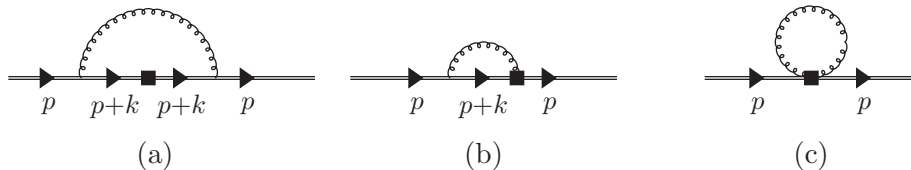


Figure 5: operator corrections.

$$\begin{aligned}
&= -\frac{4i}{3a}g_0^2 \int_k \frac{D_4^2 + \sum_{i=1}^3 G_{4i}^2}{2W + a^2\lambda^2} (\Gamma_j + ap_j \cos(k_j)) e^{-iap_4} \left( \frac{e^{-i\frac{k_4+ap_4}{2}}}{1 - e^{-i(k_4+ap_4)} + \epsilon} \right)^2 \\
&= -\frac{4i}{3a}g_0^2 \int_k \frac{D_4^2 + \sum_{i=1}^3 G_{4i}^2}{2W + a^2\lambda^2} (\Gamma_j + ap_j \cos(k_j)) (1 - iap_4) \\
&\quad \times \frac{1}{\left[ 2i \sin\left(\frac{k_4+ap_4}{2}\right) + e^{i\frac{k_4+ap_4}{2}} \epsilon \right]^2} \\
&= -\frac{4}{3}ig_0^2 p_j \int_k \frac{D_4^2 + \sum_{i=1}^3 G_{4i}^2}{2W + a^2\lambda^2} \frac{\cos(k_j)}{(2iN_4 + \epsilon M_4)^2} \tag{52}
\end{aligned}$$

$$\begin{aligned}
V_j'^0 &= -\frac{4i}{3a}g_0^2 \int_k h_{4k} h_{4l} \Delta_{kl} (\Gamma_j + ap_j \cos(k_j)) e^{-iap_4} \left( \frac{e^{-i\frac{k_4+ap_4}{2}}}{1 - e^{-i(k_4+ap_4)} + \epsilon} \right)^2 \\
&= -\frac{4i}{3a}g_0^2 \int_k h_{4k} h_{4l} \Delta_{kl} (\Gamma_j + ap_j \cos(k_j)) (1 - iap_4) \frac{1}{\left( 2i \sin\left(\frac{k_4+ap_4}{2}\right) + e^{i\frac{k_4+ap_4}{2}} \epsilon \right)^2} \\
&= -\frac{4i}{3}g_0^2 p_j \int_k \left( D_4^2 K^0 + N_4^2 \Lambda \right) \cos(k_j) \frac{1}{(2iN_4 + \epsilon M_4)^2} = \frac{1}{3}g_0^2 ip_j \int_k \Lambda \cos(k_j).
\end{aligned}$$

The ‘‘sail diagram’’ has the following expression:

$$\begin{aligned}
V_j^1 &= \frac{4}{3a}g_0^2 \int_k h_{4l} D_{lj} \cos\left(\frac{k_j}{2} + ap_j\right) \frac{e^{-i\left(\frac{k_4}{2} + ap_4\right)}}{1 - e^{-i(k_4+ap_4)} + \epsilon} = V_j^{1,\text{plaq}} + V_j'^1 \\
V_j^{1,\text{plaq}} &= \frac{4}{3a}g_0^2 \int_k \frac{G_{4j}}{2W + a^2\lambda^2} (M_j - ap_j N_j) \left(1 - i\frac{ap_4}{2}\right) \frac{1}{2i \sin\left(\frac{k_4+ap_4}{2}\right) + e^{i\frac{k_4+ap_4}{2}} \epsilon} \\
&= -\frac{4}{3a}g_0^2 p_j \int_k \frac{G_{4j} N_j}{2W + a^2\lambda^2} \frac{1}{2iN_4 + \epsilon M_4} = \frac{2}{3}g_0^2 ip_j \int_k \frac{G'_{4j} N_j}{2W + a^2\lambda^2}, \\
G_{4j} &= N_4 G'_{4j} \tag{53}
\end{aligned}$$

$$\begin{aligned}
V_j'^1 &= \frac{4}{3a}g_0^2 \int_k h_{4l} \Delta_{lj} (M_j - ap_j N_j) \left(1 - i\frac{ap_4}{2}\right) \frac{1}{2i \sin\left(\frac{k_4+ap_4}{2}\right) + e^{i\frac{k_4+ap_4}{2}} \epsilon} \\
&= -\frac{4}{3}g_0^2 p_j \int_k \left( 4D_4 N_4 N_j L_{4j} + N_4 N_j \Lambda'_j \right) N_j \frac{1}{2iN_4 + \epsilon M_4} \\
&= \frac{2}{3}g_0^2 ip_j \int_k N_j^2 \left( 4D_4 L_{4j} + \Lambda'_j \right), \quad N_4 N_j \Lambda'_j = \sum_{i=1}^3 G_{4i} \Delta_{ij}. \tag{54}
\end{aligned}$$

Note that the contribution of the sail diagram to the final result must be doubled, because the gluon leg can be attached to the static line in two different ways. Eventually the tadpole diagram is given by

$$V_j^2(\alpha_i) = -\frac{1}{2!} \frac{4}{3} ig_0^2 p_j \int_k D_{44} = -\frac{ig_0^2}{12\pi^2} p_j \left( f_3(\alpha_i = 0) + f'_3(\alpha_i = 0, c_i) \right). \tag{55}$$



We finally have

$$\langle H^{**} | O_{ij}^R | H \rangle = \frac{1}{Z_{\mathcal{D}}(\alpha_i)} \langle H^{**} | O_{ij}^B | H \rangle(\alpha_i), \quad (56)$$

where

$$Z_{\mathcal{D}}(\alpha_i) = Z_{2h}(\alpha_i) \left( 1 + \delta V(\alpha_i) \right) \quad (57)$$

$$\delta V(\alpha_i) \equiv \frac{g_0^2}{12\pi^2} \left( 2 \ln(a^2 \lambda^2) + f_4(\alpha_i) + f'_4(\alpha_i, c_i) \right) \quad (58)$$

i.e.

$$Z_{\mathcal{D}}(\alpha_i) = 1 + \frac{g_0^2}{12\pi^2} z_d(\alpha_i) \quad , \quad z_d = z_2 + f_4 + f'_4. \quad (59)$$

The numerical values of  $z_d$  are collected in Table 7 for the different kinds of static quark and gluonic actions. With the bare coupling  $g_0^2 \equiv 6/\beta$ , the tree-level Symanzik improved gauge action at  $\beta = 3.9$  and the HYP2 static quark action used in our simulations we obtain  $Z_{\mathcal{D}}(\text{tlSym}, \text{HYP2}) = 0.976$ .

|                      | $\alpha_i = 0$ | HYP1  | HYP2  |
|----------------------|----------------|-------|-------|
| $f_1$                | 7.72           | 1.64  | -1.76 |
| $f'_1(\text{tlSym})$ | 2.10           | 0.14  | 0.83  |
| $f_2$                | -12.25         | 1.60  | 9.58  |
| $f'_2(\text{tlSym})$ | -3.43          | -0.12 | -1.50 |
| $f_3$                | 12.23          | 4.12  | 5.96  |
| $f'_3(\text{tlSym})$ | -2.10          | -0.14 | -0.83 |
| $f_4$                | -12.68         | -4.95 | -0.56 |
| $f'_4(\text{tlSym})$ | 3.56           | 2.04  | 1.67  |
| $\sigma_0$           | 19.95          | 5.76  | 4.20  |
| $z_2(\text{plaq})$   | 24.48          | 2.52  | -3.62 |
| $z_2(\text{tlSym})$  | 25.81          | 2.50  | -2.96 |
| $z_d(\text{plaq})$   | 11.80          | -2.43 | -4.19 |
| $z_d(\text{tlSym})$  | 16.69          | -0.41 | -1.85 |

Table 7: numerical values of the constants  $f_1, f'_1, f_2, f'_2, f_3, f'_3, f_4, f'_4, \sigma_0, z_2$  and  $z_d$  defined in the text;  $\alpha_i = 0$  denotes the unsmearred Eichten-Hill static quark action, while HYP1 and HYP2 are defined in [25] and [27] respectively; “plaq” denotes the standard Wilson plaquette gauge action, while “tlSym” denotes the tree-level Symanzik improved gauge action.

## 5 Conclusions

We have computed the form factors  $\tau_{1/2}(1)$  and  $\tau_{3/2}(1)$  in the static limit, which describe (in this limit) the decay  $B \rightarrow D^{**}$ . This decay is presently a puzzle in the sense that sum rules

derived from QCD point towards a dominance of  $\tau_{3/2}(1)$ , while experimental indications point rather in the opposite direction. The aim of this paper has been to check the dominance of  $\tau_{3/2}(1)$  in a quantitative way.

Our final result extrapolated to the physical  $u/d$  quark mass is given in Table 6. Since we see no systematic dependence on the temporal separation  $t_0 - t_2$  except for an increase in statistical uncertainty, we keep the result at  $t_0 - t_2 = 10$ . To the statistical error we add a systematical error of 3% to account for the uncertainty in the computation of the renormalization constant  $Z_{\mathcal{D}}$ , which was computed perturbatively. We make the “guesstimate” of 100% uncertainty on  $1 - Z_{\mathcal{D}}$ , which turns out to be very small. Notice that this uncertainty does not apply to the ratio  $\tau_{3/2}(1)/\tau_{1/2}(1)$  both having the same  $Z_{\mathcal{D}}$  (cf. eqns. (25) and (26)). We have at this stage no way to estimate systematic uncertainties arising from finite lattice spacing and from finite volume. Therefore, we must consider the errors we quote as incomplete. We end up with

$$\tau_{1/2}(1) = 0.296(26) \quad , \quad \tau_{3/2}(1) = 0.526(23) \quad (60)$$

$$\frac{\tau_{3/2}(1)}{\tau_{1/2}(1)} = 1.6 \dots 1.8 \quad , \quad \left| \tau_{3/2}(1) \right|^2 - \left| \tau_{3/2}(1) \right|^2 \approx 0.17 \dots 0.21 \quad (61)$$

in fair agreement with the qualitative claim that  $\tau_{3/2}$  is significantly larger than  $\tau_{1/2}$ . Note also that Uraltsev’s sum rule is almost saturated by the ground state contributions providing  $\approx 80\%$  of the required 1/4 (cf. eqn. (1)).

This result does not differ qualitatively from the preliminary quenched computation [7]:  $\tau_{1/2} = 0.38(5)$  and  $\tau_{3/2} = 0.53(8)$ . However, we consider the result presented in this paper as standing on a much firmer ground, because it is unquenched, and because the signal is much clearer and more stable thanks to better analysis procedures. Our result (60) is also similar to the prediction of a Bakamjian-Thomas relativistic quark model [4], when using a Godfrey-Isgur interquark potential:  $\tau_{1/2} = 0.22$  and  $\tau_{3/2} = 0.54$ .

Assuming that the heavy quark limit provides reliable indications and that the standard identification of narrow  $D^{**}$  resonances is correct (i.e.  $D_1(2420)$  ( $J = 1$ ) and  $D_2^*(2460)$  ( $J = 2$ ) correspond to  $j = 3/2$  mesons) this points towards the expected dominance of the semileptonic decay of  $B$  mesons into these  $j = 3/2$  states over the decay into  $j = 1/2$  states. The latter, labeled as  $D_0^*$  ( $J = 0$ ) and  $D_1'$  ( $J = 1$ ) are identified to some broad structures, which are seen in the semileptonic  $B$  decay around similar masses (2200 MeV to 2600 MeV). Remember, however, that the predicted ratio of branching fractions  $\text{Br}(B \rightarrow D_{3/2}^{**})/\text{Br}(B \rightarrow D_{1/2}^{**})$  is mainly governed by  $(\tau_{3/2}(1)/\tau_{1/2}(1))^2$  times a rather large ratio of phase-space factors.

It is usually claimed from experiment that the decay into these broad resonances are not subdominant as compared to the narrow resonances. A recent analysis by BABAR [35, 36] finds significant  $B \rightarrow D^{(*)} \pi l \nu$ , but does not give the relative yield of narrow and broad resonances. In a recent paper by BELLE [37] the four  $D^{**}$  states are distinguished. The  $B \rightarrow D_0^* l \nu$  is observed with a comparatively large signal and, assuming the heavy quark limit to be applicable, they fit  $\tau_{3/2}(1) = 0.75$  and  $\tau_{1/2}(1) = 1.28$ . Compared to our result (60) this calls for two comments:

- (1) The  $\tau_{3/2}(1)$  shows fair agreement between theory and experiment. This is encouraging, since the narrow resonances are experimentally rather well under control, i.e. the narrow resonances are well seen.

- (2) The experimental  $\tau_{1/2}(1)$  is much larger than our prediction. Note, however, that BELLE does not see the other member of the  $j = 1/2$  doublet,  $B \rightarrow D'_1 l \nu$ . This is puzzling and the discrepancy concerning  $\tau_{1/2}(1)$  should not be taken as final.

*In view of the impressive convergence of almost all theoretical estimates of  $\tau_{1/2}(1)$  and  $\tau_{3/2}(1)$ , in view of our confidence that the result presented in this paper stands on a firm ground, we believe that one can consider as established that QCD predicts a clear dominance of the decay into  $j = 3/2$  in the static limit.*

It still remains to be solved, how to saturate the inclusive semileptonic branching ratio, in other words what to add to the  $B \rightarrow D^{(*)} l \nu$  and to the narrow  $D^{**}$  resonances. The analyses performed on Class I non-leptonic  $B \rightarrow D^{**} \pi$  decay do not find any trace of broad structures [38, 39]. Invoking factorization, theoretically well under control for this kind of process this naturally leads again to  $\tau_{1/2}(1) < \tau_{3/2}(1)$ .

Experimental work still has to be done. On the theory side, beyond doing the computation at another finer lattice spacing to be able to perform a continuum extrapolation (theoretically well defined, as recalled in Section 2), an estimate of the  $1/m_c$  corrections would help a lot. To explore that issue a promising method used to study the  $B \rightarrow D^{(*)} l \nu$  form factors at non-zero recoil [40, 41] might be helpful. The contributions of other states such as negative parity radial excitations should also be considered.

Let us conclude by insisting that the issue at clue is of important relevance: any accurate estimate of the  $V_{cb}$  parameter of the standard model will never be fully convincing as long as the “1/2 versus 3/2 puzzle” remains unsolved.

## Acknowledgments

B.B. and O.P. thank Ikaros Bigi and the other authors of [1] for many discussions on these issues and having stimulated the present work. We also thank Vladimir Galkin, Karl Jansen, Chris Michael, David Palao and Andrea Shindler for many helpful discussions.

This work has been supported in part by the EU Contract No. MRTN-CT-2006-035482, “FLAVIANet”, by the DFG Sonderforschungsbereich/Transregio SFB/TR9-03 and by the project ANR-NT-05-3-43577 (QCDNEXT).

We thank CCIN2P3 in Lyon and the Jülich Supercomputing Center (JSC) for having allocated to us computer time, which was used in this work.

## A Feynman rules

The lattice HQET action is

$$S^{\text{HQET}} = a^3 \sum_n \left( Q^\dagger(n) \left( Q(n) - U_4^{\dagger, \text{HYP}}(n - \hat{4}) Q(n - \hat{4}) \right) + a \delta m Q^\dagger(n) Q(n) \right), \quad (62)$$

where  $U_4^{\text{HYP}}(n)$  is a link built from hypercubic blocking.

We will use in the rest of this appendix the following notations taken from [42, 43, 44]:

$$\int_p \equiv \int_{-\pi/a}^{\pi/a} \frac{d^4 p}{(2\pi)^4}, \quad \int_{\vec{p}} \equiv \int_{-\pi/a}^{\pi/a} \frac{d^3 p}{(2\pi)^3}, \quad a^4 \sum_n e^{ipn} = \delta(p) \quad (63)$$

$$\int_k \equiv \int_{-\pi}^{\pi} \frac{d^4 k}{(2\pi)^4}, \quad \int_{\vec{k}} \equiv \int_{-\pi}^{\pi} \frac{d^3 k}{(2\pi)^3} \quad (64)$$

$$h(n) = \int_p e^{ipn} h(p) \quad (65)$$

$$U_\mu(n) = e^{iag_0 A_\mu^a(n)T^a} = 1 + iag_0 A_\mu^a(n)T^a - \frac{a^2 g_0^2}{2!} A_\mu^a(n)A_\mu^b(n)T^a T^b + \mathcal{O}(g_0^3) \quad (66)$$

$$U_\mu^{\text{HYP}}(n) = e^{iag_0 B_\mu^a(n)T^a} = 1 + iag_0 B_\mu^a(n)T^a - \frac{a^2 g^2}{2!} B_\mu^a(n)B_\mu^b(n)T^a T^b + \mathcal{O}(g_0^3) \quad (67)$$

$$A_\mu^a(n) = \int_p e^{ip(n+\frac{a}{2})} A_\mu^a(p), \quad B_\mu^a(n) = \int_p e^{ip(n+\frac{a}{2})} B_\mu^a(p) \quad (68)$$

$$\Gamma_\lambda = \sin(ak_\lambda) \quad (69)$$

$$c_\mu = \cos\left(\frac{a(p+p')_\mu}{2}\right), \quad s_\mu = \sin\left(\frac{a(p+p')_\mu}{2}\right) \quad (70)$$

$$M_\mu = \cos\left(\frac{k_\mu}{2}\right), \quad N_\mu = \sin\left(\frac{k_\mu}{2}\right) \quad (71)$$

$$W = 2 \sum_\lambda \sin^2\left(\frac{k_\lambda}{2}\right) \quad (72)$$

$$E^2 = \sum_{i=1}^3 N_i^2 + \frac{a^2 \lambda^2}{4}, \quad E' = 2 \operatorname{argsh}(E). \quad (73)$$

In Fourier space the action at  $\mathcal{O}(g_0^2)$  is given by

$$\begin{aligned} S^{\text{HQET}} &= \int_p \frac{1}{a} Q^\dagger(p) (1 - e^{-ip_4 a}) Q(p) + \delta m Q^\dagger(p) Q(p) \\ &+ i g_0 \int_p \int_{p'} \int_q \delta(q + p' - p) Q^\dagger(p) B_4^a(q) T^a Q(p') e^{-i(p_4 + p'_4) \frac{a}{2}} \\ &+ \frac{a g_0^2}{2!} \int_p \int_{p'} \int_q \int_r \delta(q + r + p' - p) Q^\dagger(p) B_4^a(q) B_4^b(r) T^a T^b Q(p') e^{-i(p_4 + p'_4) \frac{a}{2}}. \end{aligned} \quad (74)$$

The block gauge fields  $B_\mu^a$  can be expressed in terms of the usual gauge fields:

$$B_\mu = \sum_{n=1}^{\infty} B_\mu^{(n)}, \quad (75)$$

where  $B_\mu^{(n)}$  contains  $n$  factors of  $A$ . At next to leading order, it was shown that we only need  $B_\mu^{(1)}$  [45]:

$$B_\mu^{(1)}(k) = \sum_\nu h_{\mu\nu}(k) A_\nu(k) \quad (76)$$

$$h_{\mu\nu}(k) = \delta_{\mu\nu}D_\mu(k) + (1 - \delta_{\mu\nu})G_{\mu\nu}(k) \quad (77)$$

$$D_\mu(k) = 1 - d_1 \sum_{\rho \neq \mu} N_\rho^2 + d_2 \sum_{\rho < \sigma, \rho, \sigma \neq \mu} N_\rho^2 N_\sigma^2 - d_3 N_\rho^2 N_\sigma^2 N_\tau^2 \quad (78)$$

$$G_{\mu\nu}(k) = N_\mu N_\nu \left( d_1 - d_2 \frac{N_\rho^2 + N_\sigma^2}{2} + d_3 \frac{N_\rho^2 N_\sigma^2}{3} \right) \quad (79)$$

$$d_1 = \frac{2}{3}\alpha_1(1 + \alpha_2(1 + \alpha_3)) \quad , \quad d_2 = \frac{4}{3}\alpha_1\alpha_2(1 + 2\alpha_3) \quad , \quad d_3 = 8\alpha_1\alpha_2\alpha_3. \quad (80)$$

The Feynman rules are the following:

|                                       |  |
|---------------------------------------|--|
| heavy quark propagator                | $a(1 - e^{-ip_4 a} + \epsilon)^{-1}$   |
| vertex $V_{\mu, hhg}^a(p, p')$        | $-ig_0 T^a \delta_{\mu 4} \sum_\rho h_{\mu\rho} e^{-i(p_4 + p'_4) \frac{a}{2}}$  |
| vertex $V_{\mu\nu, hhgg}^{ab}(p, p')$ | $-\frac{1}{2} a g_0^2 \delta_{\mu 4} \delta_{\nu 4} \sum_{\rho, \sigma} h_{\mu\rho} h_{\nu\sigma} \{T^a, T^b\} e^{-i(p_4 + p'_4) \frac{a}{2}}$ |
| gluon propagator in the Feynman gauge | $a^2 (C_0^{-1} \delta_{\mu\nu} \delta^{ab} (2W + a^2 \lambda^2)^{-1} + \Delta_{\mu\nu})$   |

Note that  $p'$  and  $p$  are the in-going and the out-going fermion momenta, respectively. We also introduce an infrared regulator  $\lambda$  for the gluon propagator. We symmetrize the vertex  $V_{\mu\nu, hhgg}^{ab}$  by introducing the anti-commutator of the  $SU(3)$  generators normalized by a factor  $1/2$ . The gluon propagator and the vertices are defined with the  $A$  field. At one-loop the infrared regulator to the gluon propagator that we have chosen is legitimate, because no three-gluon vertex is involved.

## References

- [1] I. I. Bigi *et al.*, “Memorino on the ‘1/2 vs. 3/2 puzzle’ in  $\bar{B} \rightarrow l \bar{\nu} X_c$  – a year later and a bit wiser,” *Eur. Phys. J. C* **52**, 975 (2007) [arXiv:0708.1621 [hep-ph]].
- [2] A. Le Yaouanc, L. Oliver, O. Pene and J. C. Raynal, “New heavy quark limit sum rules involving Isgur-Wise functions and decay constants,” *Phys. Lett. B* **387**, 582 (1996) [arXiv:hep-ph/9607300].
- [3] N. Uraltsev, “New exact heavy quark sum rules,” *Phys. Lett. B* **501**, 86 (2001) [arXiv:hep-ph/0011124].
- [4] V. Morenas, A. Le Yaouanc, L. Oliver, O. Pene and J. C. Raynal, “Quantitative predictions for  $B$  semileptonic decays into  $D$ ,  $D^*$  and the orbitally excited  $D^{**}$  in quark models a la Bakamjian-Thomas,” *Phys. Rev. D* **56** (1997) 5668 [arXiv:hep-ph/9706265].
- [5] D. Ebert, R. N. Faustov and V. O. Galkin, “Exclusive semileptonic decays of  $B$  mesons to orbitally excited  $D$  mesons in the relativistic quark model,” *Phys. Lett. B* **434**, 365 (1998) [arXiv:hep-ph/9805423].
- [6] D. Ebert, R. N. Faustov and V. O. Galkin, “Heavy quark  $1/m(Q)$  contributions in semileptonic  $B$  decays to orbitally excited  $D$  mesons,” *Phys. Rev. D* **61**, 014016 (2000) [arXiv:hep-ph/9906415].

- [7] D. Becirevic *et al.*, “Lattice measurement of the Isgur-Wise functions  $\tau_{1/2}$  and  $\tau_{3/2}$ ,” Phys. Lett. B **609**, 298 (2005) [arXiv:hep-lat/0406031].
- [8] M. Crisafulli, V. Gimenez, G. Martinelli and C. T. Sachrajda, “First lattice calculation of the  $B$  meson binding and kinetic energies,” Nucl. Phys. B **457**, 594 (1995) [arXiv:hep-ph/9506210].
- [9] M. Della Morte, N. Garron, M. Papinutto and R. Sommer, “Heavy quark effective theory computation of the mass of the bottom quark,” JHEP **0701**, 007 (2007) [arXiv:hep-ph/0609294].
- [10] K. Jansen, C. Michael, A. Shindler and M. Wagner [ETM Collaboration], “Static-light meson masses from twisted mass lattice QCD,” PoS **LATTICE2008**, 122 (2008) [arXiv:0808.2121 [hep-lat]].
- [11] K. Jansen, C. Michael, A. Shindler and M. Wagner [ETM Collaboration], “The static-light meson spectrum from twisted mass lattice QCD,” JHEP **0812**, 058 (2008) [arXiv:0810.1843 [hep-lat]].
- [12] N. Isgur and M. B. Wise, “Weak decays of heavy mesons in the static quark approximation,” Phys. Lett. B **232**, 113 (1989).
- [13] N. Isgur and M. B. Wise, “Weak transition form-factors between heavy mesons,” Phys. Lett. B **237**, 527 (1990).
- [14] N. Isgur and M. B. Wise, “Excited charm mesons in semileptonic  $\bar{B}$  decay and their contributions to a Bjorken sum rule,” Phys. Rev. D **43**, 819 (1991).
- [15] E. Eichten and B. R. Hill, “An effective field theory for the calculation of matrix elements involving heavy quarks,” Phys. Lett. B **234**, 511 (1990).
- [16] A. K. Leibovich, Z. Ligeti, I. W. Stewart and M. B. Wise, “Semileptonic  $B$  decays to excited charmed mesons,” Phys. Rev. D **57**, 308 (1998) [arXiv:hep-ph/9705467].
- [17] N. Isgur and M. B. Wise, “Excited charm mesons in semileptonic  $\bar{B}$  decay and their contributions to a Bjorken sum rule,” Phys. Rev. D **43**, 819 (1991).
- [18] Ph. Boucaud *et al.* [ETM Collaboration], “Dynamical twisted mass fermions with light quarks,” Phys. Lett. B **650**, 304 (2007) [arXiv:hep-lat/0701012].
- [19] C. Urbach [ETM Collaboration], “Lattice QCD with two light Wilson quarks and maximally twisted mass,” PoS **LAT2007**, 022 (2007) [arXiv:0710.1517 [hep-lat]].
- [20] Ph. Boucaud *et al.* [ETM collaboration], “Dynamical twisted mass fermions with light quarks: simulation and analysis details,” Comput. Phys. Commun. **179**, 695 (2008) [arXiv:0803.0224 [hep-lat]].
- [21] P. Weisz, “Continuum Limit Improved Lattice Action For Pure Yang-Mills Theory. 1,” Nucl. Phys. B **212**, 1 (1983).
- [22] R. Frezzotti, P. A. Grassi, S. Sint and P. Weisz [Alpha collaboration], “Lattice QCD with a chirally twisted mass term,” JHEP **0108**, 058 (2001) [arXiv:hep-lat/0101001].

- [23] R. Frezzotti and G. C. Rossi, “Chirally improving Wilson fermions. I: O(a) improvement,” JHEP **0408**, 007 (2004) [arXiv:hep-lat/0306014].
- [24] A. Shindler, “Twisted mass lattice QCD,” Phys. Rept. **461**, 37 (2008) [arXiv:0707.4093 [hep-lat]].
- [25] A. Hasenfratz and F. Knechtli, “flavour symmetry and the static potential with hypercubic blocking,” Phys. Rev. D **64**, 034504 (2001) [arXiv:hep-lat/0103029].
- [26] M. Della Morte *et al.*, “Lattice HQET with exponentially improved statistical precision,” Phys. Lett. **B581**, 93, (2004) [arXiv:hep-lat/0307021].
- [27] M. Della Morte, A. Shindler and R. Sommer, “On lattice actions for static quarks,” JHEP **0508**, 051 (2005) [arXiv:hep-lat/0506008].
- [28] S. Gusken, “A study of smearing techniques for hadron correlation functions,” Nucl. Phys. Proc. Suppl. **17** (1990) 361.
- [29] M. Albanese *et al.* [APE Collaboration], “Glueball masses and string tension in lattice QCD,” Phys. Lett. B **192**, 163 (1987).
- [30] M. Lüscher and U. Wolff, “How to calculate the elastic scattering matrix in two-dimensional quantum field theories by numerical simulation,” Nucl. Phys. B **339**, 222 (1990).
- [31] B. Blossier, M. Della Morte, G. von Hippel, T. Mendes and R. Sommer, “On the generalized eigenvalue method for energies and matrix elements in lattice field theory,” arXiv:0902.1265 [hep-lat].
- [32] C. Gattringer, “Excited hadrons on the lattice - state of the art and future challenges,” arXiv:0711.0622 [hep-lat].
- [33] B. Blossier, A. Le Yaouanc, V. Morenas and O. Pene, “Lattice renormalization of the static quark derivative operator,” Phys. Lett. B **632**, 319 (2006) [Erratum-ibid. B **645**, 476 (2007)] [arXiv:hep-lat/0507024].
- [34] R. Horsley, H. Perlt, P. E. L. Rakow, G. Schierholz and A. Schiller [QCDSF Collaboration], “One-loop renormalisation of quark bilinears for overlap fermions with improved gauge actions,” Nucl. Phys. B **693**, 3 (2004) [Erratum-ibid. B **713**, 601 (2005)] [arXiv:hep-lat/0404007].
- [35] B. Aubert *et al.* [BABAR Collaboration], “Measurement of the branching fractions of exclusive  $\bar{B} \rightarrow D/D^*/D^{(*)} \pi l^- \bar{\nu}_l$  decays in events tagged by a fully reconstructed  $B$  meson,” arXiv:0708.1738 [hep-ex].
- [36] B. Aubert *et al.* [BABAR Collaboration], “Measurement of the branching fractions of  $\bar{B} \rightarrow D^{**} l^- \bar{\nu}_l$  decays in events tagged by a fully reconstructed  $B$  meson,” Phys. Rev. Lett. **101**, 261802 (2008) [arXiv:0808.0528 [hep-ex]].
- [37] D. Liventsev *et al.* [Belle Collaboration], “Study of  $B \rightarrow D^{**} l \nu$  with full reconstruction tagging,” Phys. Rev. D **77**, 091503 (2008) [arXiv:0711.3252 [hep-ex]].

- [38] K. Abe *et al.* [Belle Collaboration], “Study of  $B_0 \rightarrow \bar{D}_0^{(*)} \pi^+ \pi^-$  decays,” arXiv:hep-ex/0412072.
- [39] B. Aubert *et al.* [BABAR Collaboration], “Measurement of the absolute branching fractions  $B \rightarrow D \pi, D^* \pi, D^{**} \pi$  with a missing mass method,” Phys. Rev. D **74**, 111102 (2006) [arXiv:hep-ex/0609033].
- [40] G. M. de Divitiis, R. Petronzio and N. Tantalo, “Quenched lattice calculation of semileptonic heavy-light meson form factors,” JHEP **0710**, 062 (2007) [arXiv:0707.0587 [hep-lat]].
- [41] G. M. de Divitiis, R. Petronzio and N. Tantalo, “Quenched lattice calculation of the vector channel  $B \rightarrow D^* l \nu$  decay rate,” Nucl. Phys. B **807**, 373 (2009) [arXiv:0807.2944 [hep-lat]].
- [42] S. Capitani, “Lattice perturbation theory,” Phys. Rept. **382**, 113 (2003) [arXiv:hep-lat/0211036].
- [43] T. A. DeGrand, “One loop matching coefficients for a variant overlap action and some of its simpler relatives,” Phys. Rev. D **67**, 014507 (2003) [arXiv:hep-lat/0210028].
- [44] W. J. Lee and S. R. Sharpe, “Perturbative matching of staggered four-fermion operators with hypercubic fat links,” Phys. Rev. D **68**, 054510 (2003) [arXiv:hep-lat/0306016].
- [45] W. J. Lee, “Perturbative improvement of staggered fermions using fat links,” Phys. Rev. D **66**, 114504 (2002) [arXiv:hep-lat/0208032].